

Gallium-based thermal interface material with high compliance and wettability

Yunxia Gao · Jing Liu

Received: 13 March 2012 / Accepted: 13 March 2012 / Published online: 30 March 2012
© Springer-Verlag 2012

Abstract This study reports a gallium-based thermal interface material (GBTIM) consisting of gallium oxides dispersed uniformly into the 99 % gallium metal. The wettability of GBTIM with other materials is disclosed and compared. The thermal conductivity of GBTIM measured by a computer-controlled Mathis TCi thermal analyzer is $\sim 13.07 \text{ W m}^{-1} \text{ K}^{-1}$ at room temperature, which is significantly higher than that of conventional thermal greases. An experimental facility is described to measure the thermal resistance across the GBTIM under steady-state conditions and the thermal interface resistance is measured as low as $2.6 \text{ mm}^2 \text{ kW}^{-1}$ with a pressure of 0.05 MPa, which is an order lower than that of the best commercialized thermal greases. Further, the GBTIM is formed into a desired shape to enhance thermal transfer, such as semi-liquid paste or thermal pad, which can be cut into a required shape.

1 Introduction

With the trend of the rapid progress of the highly integrated and minimized electronics, power density of electronic components has increased year by year. In response to the size limitations and strict reliability requirements, such electronic systems generally require cooling a high power density through a limited temperature drop from device junction to a cooling system. Hence, heat removal remains a big challenge for the utilization of electronic devices with high performance, spanning from multicore processor, high

brightness light emitting diodes (LEDs), to advanced military avionics [1–3]. In order to achieve the necessary cooling, using an efficient cooling system and high thermal conductive coolant materials is an effective way. In addition, thermal interface materials (TIMs) with high performance used to form a thermal joint between an electronic component, such as a chip and a cooling system, are also found to be more important and critical [4–6].

Heat transfer between solid interfaces can be of great importance in many applications. However, solid–solid interfaces usually have relatively high thermal resistance, especially the high contact resistance which is due to the surface roughness of both surfaces which prevents perfect contact between the surfaces. For example, the contact resistance of a thermal interface consisting of bare silicon to silicon contact is on the order of $100 \text{ mm}^2 \text{ kW}^{-1}$ [7, 8]. To solve this problem, TIMs can be adopted to reduce the contact resistance between solid contacts. Generally speaking, a thermal interface material should have high thermal conductivity and sufficient compliance to assure great conformability to the solid surfaces. Such thermal interface materials can significantly enhance the contact between solid surfaces and thus reduce the contact resistance.

So far, a wide range of TIMs have been investigated: thermal fluids, thermal greases or pastes, phase change materials, solders, thermal pads, thermally conductive adhesives. Thermal greases can have thermal interface resistance ranging between 20 and $100 \text{ mm}^2 \text{ kW}^{-1}$ when filled with conductive powders, while it can be as low as $6 \text{ mm}^2 \text{ kW}^{-1}$ when filled with Na_2SiO_3 and BN [9]. Currently, research on thermal interface materials has focused on polymer-based gels and it can achieve values in the range of $40\text{--}80 \text{ mm}^2 \text{ kW}^{-1}$ [9], in some improved gels using more advanced fillers such as graphite nanoplatelets [10], or the fabrication of thermal interface materials using carbon nan-

Y. Gao · J. Liu (✉)
Technical Institute of Physics and Chemistry, Chinese Academy of Sciences, P.O. Box 2711, Beijing 100190, P.R. China
e-mail: jliu@mail.ipc.ac.cn
Fax: +86-10-82543767

otube arrays (CNTs) [11–13], a thermal interface resistance can be as low as $19.8 \text{ mm}^2 \text{ kW}^{-1}$ [12].

As is well known, the thermal conductivity of a metal is much higher than that of general inorganic/organic materials, such as thermal fluid, silicone oil, and any other organic fluids. Thus, if a certain liquid metal or its alloys with a low melting point are utilized as a thermal interface material, a much higher heat transfer capacity than that of traditional TIMs can be obtained. Hamdan et al. present a thermal interface material consisting of an array of mercury microdroplets deposited on a silicon die [14]. The thermal interface resistance was measured as low as $0.235 \text{ mm}^2 \text{ kW}^{-1}$. Compared with mercury, gallium and its alloys are nontoxic and safe. In fact, gallium and its alloys due to their favorable properties, such as nontoxic, low melting point, high thermal conductivity and so on, have been proposed by Liu and Zhou in 2002 to be used for the thermal management of computer chips and got more valuable achievement [15–19]. Meantime, International Business Machines (IBM) company proposed a liquid metal matrix thermal paste comprised a dispersion of thermally conductive particles in a low melting temperature liquid metal matrix such as gallium or its alloys [20]. However, the wettability of liquid metal thermal paste with other materials has not been improved fundamentally and there are currently few publications concerning this critical issue, which, however, seriously restricts the practical value of such TIM.

In this paper, the gallium-based thermal interface material (GBTIM) retaining its semi-liquid state permanently and indefinitely under normal operating conditions and environment was prepared by oxidation reaction method aiming to find the highly compliant thermal interface material, which can actually be used in reality. The comprehensive experiments demonstrate that the GBTIM shows an excellent wettability with many materials because of the existence of gallium oxides. The mechanisms dominating the phenomenon were preliminarily disclosed and interpreted. The thermal properties including thermal conductivity and thermal interface resistance of GBTIM were studied.

2 Experimental setup

2.1 Preparation of GBTIM

Gallium metal with a purity of 99.99 percent was used as raw material to prepare GBTIM. A certain amount of gallium was melted and weighted. The detailed synthesis procedures were outlined respectively as follows:

Firstly, the weighted gallium was added into beaker and stirred using a magnetic stirrer. Then 10 ml 30 % NaOH solution was added slowly to clean the metals. The mixture was stirred at room temperature for short periods of time;

the contents of the beaker had both an aqueous phase and a metallic phase. Then, the gallium was separated from the mixture and stirred constantly in air at room temperature to be oxidized. As is well known, the oxide layer forms easily and prevents the gallium to be oxidized further. However, the vigorous stirring broke the oxide layer so that more and more gallium metal was further oxidized. The viscosity of mixture increased gradually with the amount of gallium oxides. After being vigorously stirred for periods of time, GBTIM can be obtained with a suitable viscosity, being composed of gallium metal and gallium oxide dispersed uniformly in gallium metal. It is worth to mention that in this experiment, the experimental parameters such as amount of gallium, stirring time and stirring speed should be tightly controlled.

2.2 Characterization of GBTIM

X-ray powder diffraction analyses (Termed as XRD) were performed on a BRUKER D8 ADVANCE X-ray powder diffractometer with CuK α radiation (graphite monochromator). The scanning step width of 0.031 and the scanning rate of 0.031 s^{-1} were applied to record the patterns in the 2θ range of 10° to 80° . The component analysis of specimen was characterized by Energy-Dispersive Spectroscopy spectra termed as EDS (FESEM, S4300, Hitachi).

Thermal conductivity measurements of GBTIM were performed in air by using a computer-controlled Mathis TCi thermal analyzer in the range of 0 to $100 \text{ W m}^{-1} \text{ K}^{-1}$. Prior to each measurement, the sample was stabilized at constant temperature for at least 1 hour to ensure thermal equilibrium.

Thermal interface resistance measurements were performed with 4 different heating powers of 40, 60, 80 and 100 W, respectively. Heating power of the source was calculated by measured input voltage and current. Three temperatures, for the upper copper block T1, lower copper block T2 and ambient T3, were measured with an accuracy $\pm 0.5 \text{ }^\circ\text{C}$ by T-type thermocouples. All the data were recorded using Agilent 34972A, USA. Temperatures were obtained when the system got stabilized.

3 Results and discussion

Figure 1 shows the Energy-Dispersive Spectroscopy (EDS) spectra for the gallium metal and the prepared GBTIM using the above method. It can be seen that the two samples consist of three elements: gallium, oxygen and carbon. The amount of oxygen in GBTIM increases apparently compared with that of Ga sample as shown in Fig. 1(b), which may be attributed to the oxidation reaction of Ga when it was stirred for a long time in air. As is well known, the amount of oxygen and carbon cannot be accurately measured by EDS.

Fig. 1 Energy-Dispersive Spectroscopy spectra of Ga, O and C elements in the (a) gallium and (b) GBTIM specimens prepared by stirred gallium metal in air at room temperature for periods of time

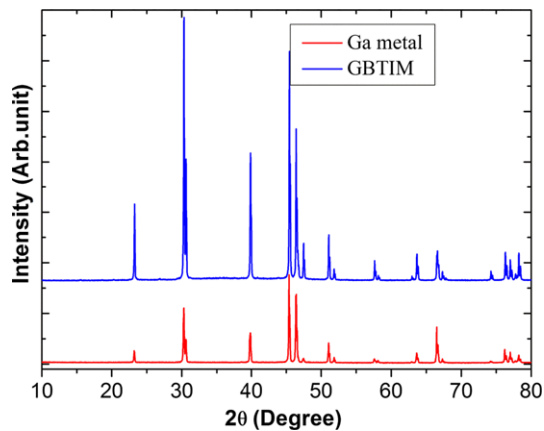
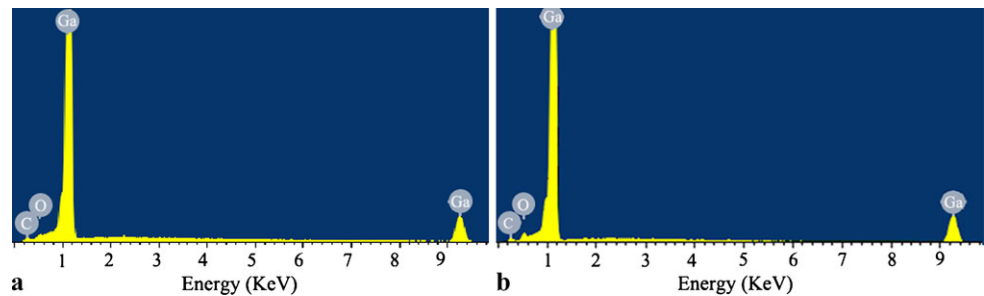


Fig. 2 Powder XRD patterns of gallium metal and GBTIM

Therefore, the accurate amount of gallium oxide in GBTIM will be discussed in the following section.

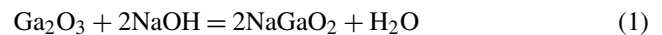
Figure 2 shows the powder XRD patterns of gallium metal and the prepared GBTIM using the above method, respectively. X-ray diffraction of gallium and GBTIM indicates the same composition of gallium (JCPDS 65-2493), which is orthorhombic, and the space group is $Cmca$. Generally speaking, the XRD patterns of content cannot be measured when its amount is less than 5 wt%. Hence combined with the results of Energy-Dispersive Spectroscopy spectra shown in Fig. 1, we think that only a small part of gallium is oxidized when stirred in air for a long time. A small amount of gallium oxides generated by stirring continuously in air disperses in gallium metal and increases the viscosity and wettability of GBTIM [21].

For a further confirmation of the composition of GBTIM, two experiments were carried out. One was in changing the experimental atmosphere as high vacuum. The gallium metal and a magnetic stirrer were sealed in quartz ware with a high vacuum of about 5×10^{-5} Pa as shown in Fig. 3(a). In the other one the prepared GBTIM was cleaned by 30 % NaOH solution at room temperature as shown in Fig. 3(b) and (c). The results are outlined in the following.

The quartz ware was put on the mixing platform and stirred. After the same periods of time, the viscosity and wettability of sample are the same as those of pure gallium metal, but totally different from those of GBTIM pre-

pared in air. The reason can be that the high vacuum of 5×10^{-5} Pa in quartz ware cannot supply sufficient oxygen for oxidation reaction of gallium to take place. More importantly, the components of GBTIM consisting of gallium metal and gallium oxide can be proved effective in this experiment.

Figure 3(b) and (c) shows respectively the morphology of GBTIM and GBTIM which is cleaned by 30 % NaOH solution for a period of time. It can be seen that the viscosity of GBTIM rapidly diminishes with cleaning time, and the fluidity is the same as that of liquid gallium. Here, the amount of sample was weighted before and after cleaning with NaOH solution. The amount of gallium oxides can be calculated as 1 wt%, which is in good agreement with the results of XRD and EDS. The possible reaction in this process can be described as follows:



In a thermal interface material, the wettability with other materials plays an important role in heat transfer. We observed the wettability of GBTIM with copper, stainless steel and silicon. For comparison, the wettability of gallium metal with copper is studied.

Prior to the experiments, the copper, stainless steel and silicon were cleaned several times by ethanol and de-ionized water with an ultrasonic frequency of 100 Hz. Figure 4(a) shows the wettability of gallium metal with copper, which is rather poor. That is, the gallium droplets easily run over because of the high surface tension of about 0.708 N m^{-1} at $29.8 \text{ }^\circ\text{C}$ [22]. Figure 4(b)–(d) presents the wettability of GBTIM with copper, stainless steel and silicon, respectively. As shown in the figure, the wettability of GBTIM is apparently improved and the thin layer can be painted uniformly on different materials, which may be explained by the existence of gallium oxide in GBTIM. Some researchers have observed that a number of different materials would be wetted by oxidized gallium or alloys [21]. The better wettability of GBTIM can reduce effectively the thermal contact resistance at the interface, which realizes the application of liquid metal used as thermal interface material in thermal management, especially in high power electronic devices.

Fig. 3 (a) The gallium sealed in quartz ware with a high vacuum of 5×10^{-5} Pa; (b) Morphology of GBTIM; (c) GBTIM was cleaned by 30 % NaOH solution for a period of time

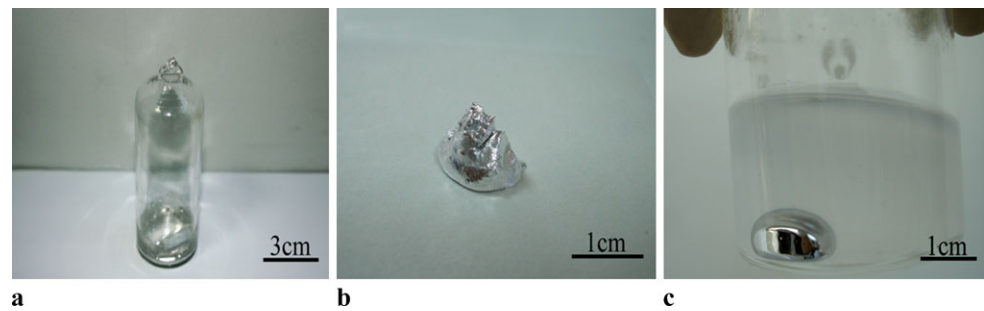
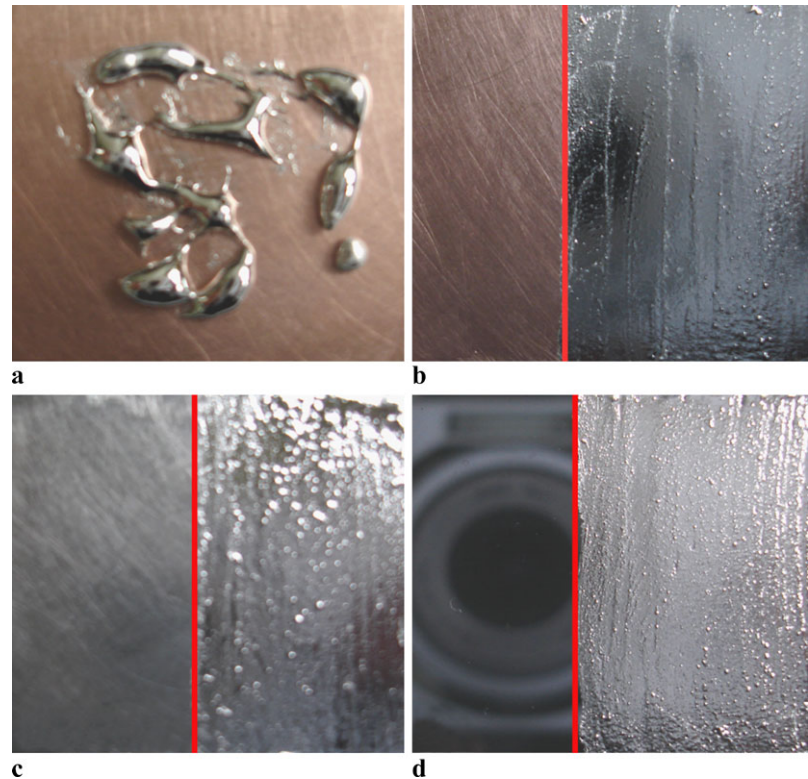


Fig. 4 Wettability of gallium metal with copper (a), GBTIM with copper (b), stainless steel (c) and silicon (d). The red line stands for the boundary



In order to achieve the cooling requirement, GBTIM must possess a high thermal conductivity which is determined by Mathis TCi thermal analyzer. After measurements for 8 times, the thermal conductivity of GBTIM is about $13.07 \text{ W m}^{-1} \text{ K}^{-1}$ at room temperature. In general, the thermal conductivity of gallium metal is about $29.4 \text{ W m}^{-1} \text{ K}^{-1}$ at $50 \text{ }^\circ\text{C}$ [23]. Namely, a small amount of gallium oxide can apparently decrease the thermal conductivity of gallium. However, it is still significantly higher than that of currently commercialized thermal grease which has the best thermal conductivity of $7 \text{ W m}^{-1} \text{ K}^{-1}$ when filled with some metal nanoparticles [24].

To measure the thermal interface resistance of GBTIM, the experimental apparatus is established as shown in Fig. 5. The entire experimental setup is mainly composed of three parts: the heat source, GBTIM, and the cooler system. Heat source is simulated by a heating rod and a copper block, with heat dissipation area $30 \text{ mm} \times 40 \text{ mm}$ designed to con-

tact with the material to be measured. The cooler system is formed with a copper block, heat sink and fan. The copper block is connected to heat sink using silicone grease. The outer-surface of the aluminum heat sink is cooled by air. Heat flux across the copper block and GBTIM, and the thermal interface resistance, can be obtained by the temperature difference of two sides of GBTIM. For reducing the heat loss, the insulated cotton and plastic foam are used to wrap the copper blocks. The heat loss estimated by the temperature difference of copper blocks with the ambient is less than 1 %.

Heat flux across the block is measured using the steady-state temperature difference ($\Delta T = T_1 - T_2$) between the two sections (Sect. 1 and Sect. 2 as shown in Fig. 6(a)). From these data, the thermal resistance of the sample is calculated as

$$R_{\text{total}} = \frac{A(T_1 - T_2)}{Q} \quad (2)$$

where Q is the total power, A is the sample area, and $T1$ and $T2$ represent the temperatures of the two blue points on the upper Cu block and lower Cu block, respectively.

As can be seen in the equivalent resistance model (Fig. 6(b)), the measurement discussed previously encompasses all the resistance components of the structure, including the conductive thermal resistances of upper and lower copper blocks (R_{Cu1} and R_{Cu2}) and the thermal interface

resistance of GBTIM. Hence the total thermal resistance between the two sections is

$$R_{total} = R_{Cu1} + R_{GBTIM(Interface)} + R_{Cu2} \tag{3}$$

As is well known, the conductive thermal resistances of copper block can be calculated as

$$R_{Cu} = R_{Cu1} + R_{Cu2} = \frac{\Delta x}{\lambda} = \frac{\Delta x_1}{\lambda} + \frac{\Delta x_2}{\lambda} \tag{4}$$

where Δx_1 and Δx_2 are the distances from Sect. 1 or Sect. 2 to the interface, respectively, as shown in Fig. 6(a), and λ is thermal conductivity of copper. Hence we can obtain the thermal interface resistance of GBTIM by Eqs. (2), (3) and (4).

In Fig. 7(a), the temperature of heat source is plotted as a function of the heat load. As expected, temperatures of components rose with increase of the heating power. GBTIM used as thermal interface material can decrease effectively the temperature of components, especially with a pressure of 0.05 MPa. In Fig. 7(b), the temperature difference between the two copper blocks is plotted as a function of the heat load. Here, the copper blocks contact with thermal greases and GBTIM without any pressure, and GBTIM with a pressure of 0.05 MPa, respectively. It can be seen that the temperature difference of two copper blocks with GBTIM as thermal interface material is smaller than that with thermal greases as thermal interface materials. Moreover, the temperature difference decreases with increasing pressure, which is consistent behavior for most thermal interface materials. It also shows that GBTIM provides a better contact

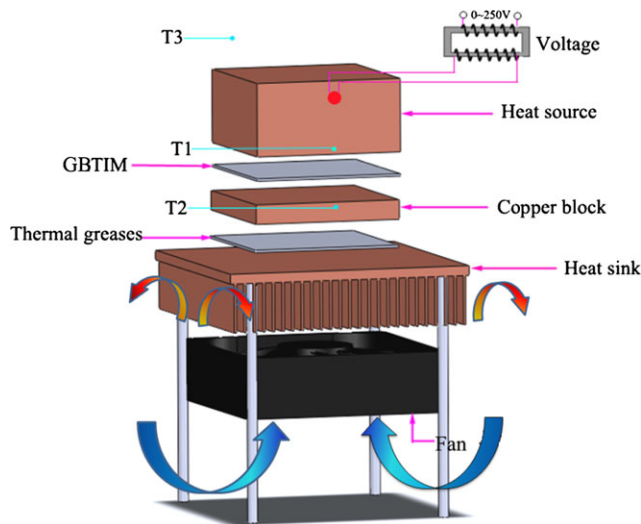


Fig. 5 Experimental apparatus for thermal resistance measurement. The arrows represent the flowing direction of wind

Fig. 6 Sketch map used for thermal resistance measurement and equivalent thermal resistance model. R_{Cu1} and R_{Cu2} represent the conductive thermal resistance of the upper and lower Cu blocks. R_{GBTIM} (interface) represents the thermal interface resistance of GBTIM

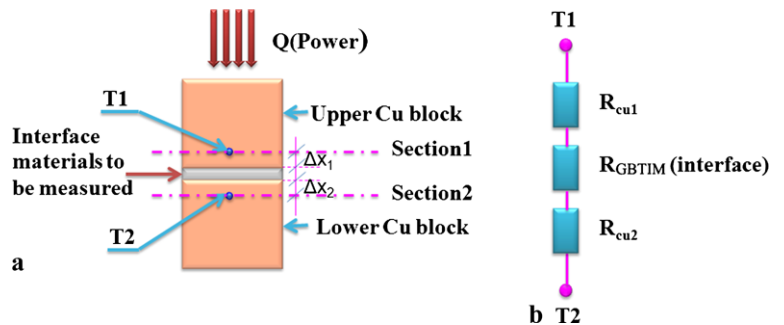


Fig. 7 Temperature of the heat source (a) and temperature difference (b) between the two copper blocks with the heat load

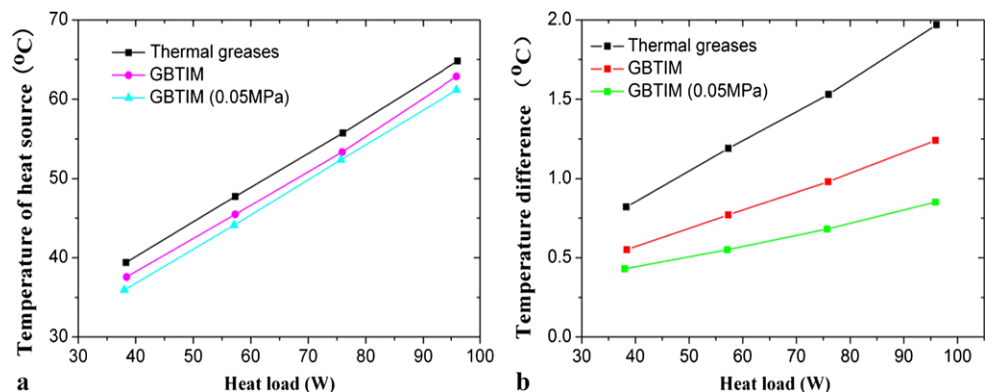


Fig. 8 Thermal infrared graph for the system using thermal greases (a) and GBTIM (b)

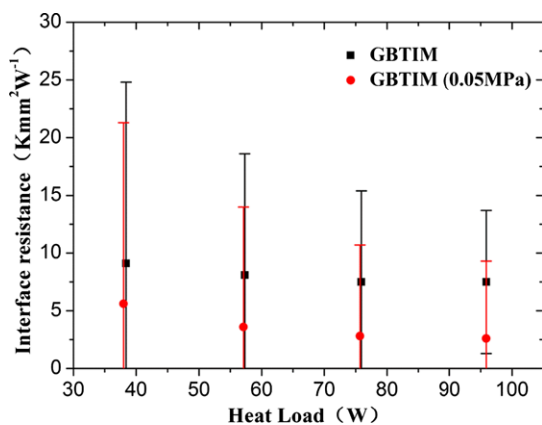
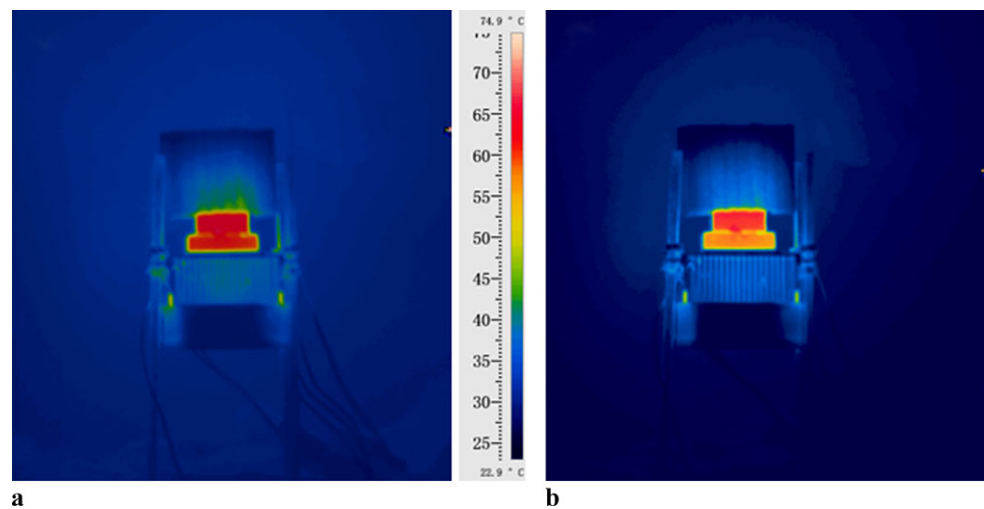


Fig. 9 Thermal interface resistance with the heat load

at increased pressure and improves the heat spreading effectiveness.

Figure 8 shows the thermal infrared graphs for the system using thermal greases and GBTIM when the heat load is around 100 W. Colors in the graphs indicate the surface temperature of the system. The emissivity is set as 0.85. The difference between temperatures obtained from the thermal infrared camera and measured by thermocouple is less than 1 °C. Since the heat source was wrapped with sufficiently insulated cotton and plastic foam, the color for heat source is a deep blue. The temperatures of the upper and lower copper blocks obtained from the infrared graph are the focus of present research. To better understand the difference between the two kinds of TIM, the temperature scales are all set from 22.9 to 74.9 °C.

The temperature of the upper copper block in Fig. 8(a) is higher than that in Fig. 8(b). Compared with thermal greases, it is confirmed, again, that GBTIM has a better heat transfer capacity due to higher thermal conductivity and lower thermal interface resistance.

Figure 9 shows the thermal interface resistance with the heat load for GBTIM without pressure and GBTIM with a pressure of 0.05 MPa. Generally speaking, constant thermal resistance values should be obtained at different heat flux. However in our case, the thermal interface resistance of GBTIM decreases from 9.1 to 7.5 mm² kW⁻¹ with increase of the heat load. This phenomenon also appears in GBTIM under a pressure of 0.05 MPa and the interface resistance ranges from 5.6 to 2.6 mm² kW⁻¹. When the heating power is higher than 75 W, namely the temperature of GBTIM is higher than 50 °C, the thermal interface resistances achieve minimized values. This can be explained by the fluidity of GBTIM. The melting point of GBTIM is measured as 30.0 °C, which is the same as the melting point of gallium metal. The GBTIM mobility is improved and minimizes thermal contact resistance under increasing heat flux by filling voids in the interfaces.

Successful thermal management requires perfect TIMs that connect the chip and the heat sink. These materials are used to reduce or completely eliminate the air gaps from the contact interfaces by conforming to the rough and uneven mating surfaces, as shown in Fig. 10(b) and (c). This is because the TIM generally possesses a higher thermal conductivity than the interfacial gas (air) they replace. The efficiency of the TIM in reducing the interfacial thermal resistance depends on a number of factors among which thermal conductivity of the materials and its ability to wet the mating surfaces appear to be the most significant [25]. GBTIM with a semi-liquid state exhibits higher thermal conductivity and better wettability of rough surfaces, making it to fill all the gaps between two solid surfaces as shown in Fig. 10(c), which can effectively reduce thermal contact resistance and thermal conductive resistance and enhance the heat spread of electronic components.

The liquid metal thermal interface material acts as a high thermal conductive medium which is formed into a desired

Fig. 10 Contributions of thermal contact resistance and thermal conductive resistance: (a) without any TIMs, (b) with poor TIMs, and (c) with GBTIM

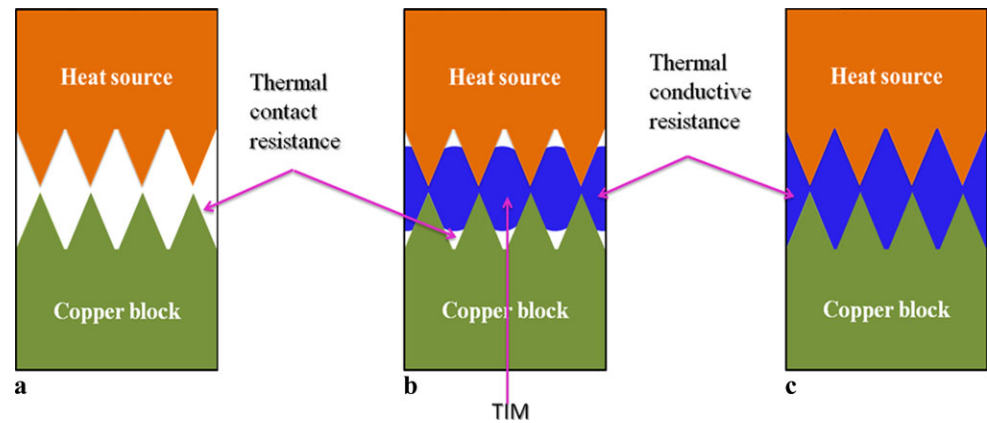
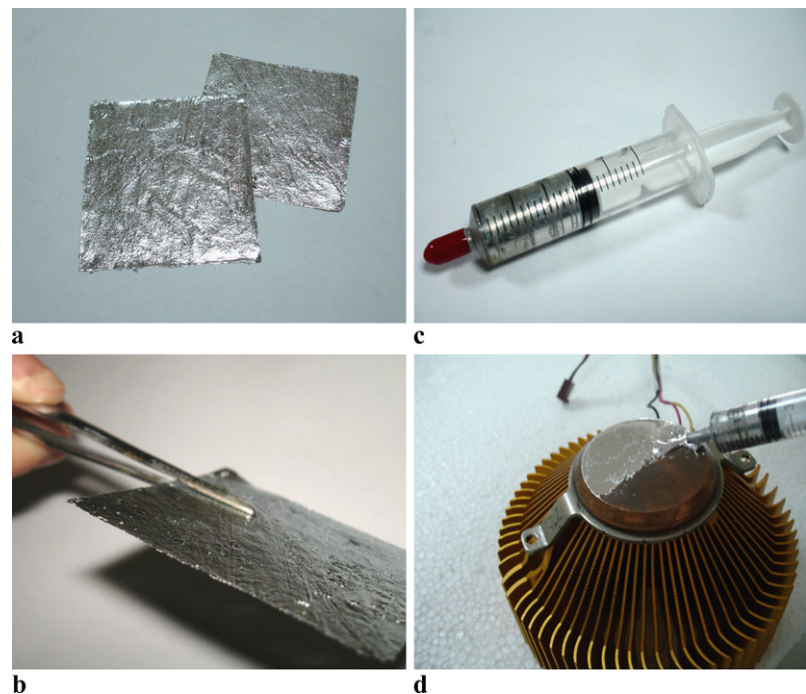


Fig. 11 Exhibition of GBTIM with different types: (a) and (b) are the photographs of GBTIM pad which can be cut into a required shape; (c) and (d) are the photographs of GBTIM which can be painted on any interface because of the liquid state



shape to enhance thermal transfer. Figure 11(a) and (b) are the photographs of GBTIM pad which can be cut into a required shape. In fact, Coollaboratory company has fabricated a kind of liquid metal pad which has a higher melting point of 58 °C [26]. However, for GBTIM, when the heat fluxes across the interface, the pad will be melt at about 30 °C and fill all the gaps, thus enhancing the heat transfer effectively. The GBTIM with a semi-liquid state was encased into the injector as shown in Fig. 11(c) and (d). It melts with just less heating and can be easily painted on any interface.

From the viewpoint of application, GBTIM consists of at least 99 % gallium metal, which is absolutely nontoxic and has a high wettability for several materials, and provides an effective and realizable way to be used as TIMs in cooling high power dissipation components in conjunction with a conventional fluid/wind cooling system. In addition,

the carbon nanotubes and nanoparticles with higher thermal conductivities including Ag, Au and Cu can be added into GBTIM to further decrease the thermal interface resistance, thus enhancing the heat transfer.

4 Conclusion

In summary, this work presents the preparation and characterization of a gallium-based thermal interface material consisting of gallium oxides dispersed into the 99 % gallium metal. The thermal conductivity of GBTIM is about $13.07 \text{ W m}^{-1} \text{ K}^{-1}$ at room temperature. An experimental facility which measures the thermal resistance across the GBTIM under steady-state conditions is described. A thermal interface resistance as low as $2.6 \text{ mm}^2 \text{ kW}^{-1}$ with a pressure of 0.05 MPa was measured, which is much lower

than that of the best commercialized thermal greases. The GBTIM is formed into a desired shape to enhance thermal transfer, such as semi-liquid paste or thermal pad, which can be cut into a required shape. Liquid metal thermal interface materials are considered to be the next-generation high-performance heat transfer medium and are believed to have remarkable advantages over already commercialized thermal interface materials with regard to higher thermal conductivity, lower thermal resistance, and better adhesion.

Acknowledgements The authors acknowledge the valuable discussions with Prof. Yixin Zhou, Mr. Peipei Li, Ms. Haiyan Li and Mr. Yueguang Deng of Technical Institute of Physics and Chemistry, Chinese Academy of Sciences.

References

1. J. Donald, M. Martonosi, in *Proceedings of the 33rd International Symposium on Computer Architecture (ISCA)*, vol. 78 (2006)
2. T. Treurniet, V. Lammens, in *22nd IEEE SEMI-THERM Symposium*, vol. 173 (2006)
3. I. Mudawar, *IEEE Trans. Compon. Packag. Technol.* **24**, 122 (2001)
4. S. Whalen, M. Thompson, D. Bahr, C. Richards, R. Richards, *Sens. Actuators A* **104**, 290 (2003)
5. U. Ghoshal, S. Ghoshal, C. McDowell, L. Shi, S. Cordes, M. Farinelli, *Appl. Phys. Lett.* **80**, 3006 (2002)
6. G. Cha, Y. Sungtaek Ju, in *ASME Int. Mech. Eng. Congress. Expos. Proc.*, vol. 12, p. 927 (2010)
7. J. Xu, T.S. Fisher, *Int. J. Heat Mass Transf.* **49**, 1658 (2006)
8. H.F. Chuang, S.M. Cooper, M. Meyyappan, B.A. Cruden, *J. Nanosci. Nanotechnol.* **4**, 964 (2004)
9. D. Chung, *J. Mater. Eng. Perform.* **10**, 56 (2001)
10. A. Yu, P. Ramesh, M.E. Itkis, E. Bekyarova, R.C. Haddon, *J. Phys. Chem. C* **111**, 7565 (2007)
11. Y. Wu, C.H. Liu, H. Huang, S.S. Fan, *Appl. Phys. Lett.* **87**, 3108 (2005)
12. B.A. Cola, X. Xu, T.S. Fisher, *Appl. Phys. Lett.* **90**, 3513 (2007)
13. B.A. Cola, J. Xu, C. Cheng, X. Xu, T.S. Fisher, H. Hu, *J. Appl. Phys.* **101**, 4313 (2007)
14. A. Hamdan, A. McLanahan, R. Richards, C. Richards, *Exp. Therm. Fluid Sci.* **35**, 1250 (2011)
15. J. Liu, Y.X. Zhou, China Patent No. 02131419.5 (2002)
16. K.Q. Ma, J. Liu, *Phys. Lett. A* **361**, 252 (2007)
17. Y.G. Deng, J. Liu, *Heat Mass Transf.* **46**, 1327 (2010)
18. P.P. Li, J. Liu, *Appl. Phys. Lett.* **99**, 094106 (2011)
19. P.P. Li, J. Liu, *J. Electron. Packag.* **133**, 041009 (2011)
20. R.B. Booth, G.W. Grube, P.A. Gruber, I.Y. Khandros, R. Zingher, US Patent, No 5.198.189 (1992)
21. L.T. Taylor, J. Rancourt, US Patent, NO 5.792.236 (1998)
22. S.C. Hardy, *J. Cryst. Growth* **7**, 602 (1985)
23. T. Iida, R.I.L. Guthrie, *The Physical Properties of Liquid Metals* (Clarendon, Oxford, 1993)
24. J.P. Gwinn, R.L. Webb, *Microelectron. J.* **34**, 215 (2003)
25. M. Grujcic, C.L. Zhao, E.C. Dusel, *Appl. Surf. Sci.* **246**, 290 (2005)
26. <http://www.coollaboratory.com/en/products/>